

ALGEBRAIC BOUNDS ON THE RAYLEIGH-BÉNARD ATTRACTOR

YU CAO¹, MICHAEL S. JOLLY^{1,†}, EDRISS S. TITI², AND JARED P. WHITEHEAD³

ABSTRACT. The Rayleigh-Bénard system with stress-free boundary conditions is shown to have a global attractor in each affine space where velocity has fixed spatial average. The physical problem is shown to be equivalent to one with periodic boundary conditions and certain symmetries. This enables a Gronwall estimate on enstrophy. That estimate is then used to bound the L^2 norm of the temperature gradient on the global attractor, which, in turn, is used to find a bounding region for the attractor in the enstrophy, palinstrophy-plane. All final bounds are algebraic in the viscosity and thermal diffusivity, a significant improvement over previously established estimates. The sharpness of the bounds are tested with numerical simulations.

1. INTRODUCTION

The long-time behavior of the Rayleigh-Bénard problem was analyzed in [10, 17] for several types of boundary conditions. In that work the authors derived explicit estimates for enstrophy and the (L^2 -norm of the) temperature gradient on the global attractor for the case of no-slip boundary conditions in space dimension two. They also outlined the functional setting for the case of stress-free velocity boundary conditions (see (2.2a), (2.2b)), and mentioned that corresponding estimates can be carried out in a similar fashion. In this paper we revisit the 2D, stress-free boundary conditions case, and as in the case of rigorous bounds on the time averaged heat transport [18], we find estimates on the global attractor which are dramatically reduced from those in the no-slip boundary conditions case. We also derive estimates for the palinstrophy and H^2 -norm of the temperature.

One marked difference between no-slip and stress-free boundary conditions is that in the latter case, the system is not dissipative for general initial velocity data. This is due to the existence of steady states with arbitrarily large L^2 -norms, namely velocity of the form $u(x, t) = (c, 0)$, with zero temperature $\theta(x, t) = 0$ such as the shear-dominated flow investigated in [12]. Since, however, the spatial average is conserved for these flows, the system is dissipative within each invariant affine space of fixed horizontal velocity average. This wrinkle does not influence the estimates on the temperature or higher Sobolev norm estimates on the velocity.

The *a priori* estimates are carried out in Section 4. The key to finding sharper bounds in the stress-free case is to extend the physical domain, as done in [8], to one that is fully periodic and twice the height of the original. This makes the trilinear term vanish from the enstrophy balance, giving an easy bound that is $\mathcal{O}(\nu^{-2})$ in

Date: May 7, 2019.

2010 Mathematics Subject Classification. 35Q35, 76E06, 76F35 34D06.

Key words and phrases. Rayleigh-Bénard convection, global attractor, synchronization.

terms of the kinematic viscosity. Though the trilinear term persists when estimating the temperature gradient, we are able to avoid the exponential bound that resulted from using a uniform Gronwall lemma in [10], by using the algebraic bound on the enstrophy. We find that on the global attractor the (L^2 -norm of the) temperature gradient satisfies a bound that is $\mathcal{O}(Ra^2)$, for $Pr \sim 1$, where Ra is the Rayleigh number and Pr is the Prandtl number.

We then follow the approach in [5] for the Navier-Stokes equations (NSE) to obtain an estimate for the palinstrophy, with the temperature playing the role of the body force in the NSE. This leads to curves which bound the attractor in the enstrophy, palinstrophy-plane, with an overall bound on palinstrophy that is $\mathcal{O}(Ra^3)$ for $Pr \sim 1$. Using this palinstrophy bound, we then follow a similar procedure to find a bounding region for temperature θ in the $\|\nabla\theta\|_{L^2}^2, \|\Delta\theta\|_{L^2}^2$ -plane.

We recall from [8] in Section 5 how all of these bounds impact the practicality of data assimilation by nudging with just the horizontal component of velocity of the stress-free Rayleigh-Bénard system. The sharpness of our rigorous bounds are tested with numerical simulations over a range of Rayleigh numbers in Section 6. Simulations are also presented there to demonstrate that the nudging algorithm works for data with much less resolution than the analysis requires. This is actually what suggested we might improve on the exponential bounds in [10, 17]. All the bounds here on the attractor are algebraic in the physical parameters.

2. PRELIMINARIES

The Rayleigh-Bénard (RB) problem on the domain $\Omega_0 = (0, L) \times (0, 1)$ can be written in dimensionless form as (see, e.g., [10])

$$\frac{\partial u}{\partial t} - \nu \Delta u + (u \cdot \nabla)u + \nabla p = \theta e_2, \quad (2.1a)$$

$$\frac{\partial \theta}{\partial t} - \kappa \Delta \theta + (u \cdot \nabla)\theta = u \cdot e_2, \quad (2.1b)$$

$$\nabla \cdot u = 0, \quad (2.1c)$$

$$u(0; x) = u_0(x), \quad \theta(0; x) = \theta_0(x). \quad (2.1d)$$

In this paper, we consider the following set of boundary conditions that are stress-free on the velocity:

$$\text{in the } x_2\text{-direction: } u_2, \theta = 0 \text{ at } x_2 = 0 \text{ and } x_2 = 1, \quad (2.2a)$$

$$\frac{\partial u_1}{\partial x_2} = 0 \text{ at } x_2 = 0 \text{ and } x_2 = 1, \quad (2.2b)$$

$$\text{in the } x_1\text{-direction: } u, \theta, p \text{ are of period } L. \quad (2.2c)$$

Following [8], in the rest of this paper, we consider the equivalent formulation of problem (2.1) subject to the fully periodic boundary conditions on the extended domain $\Omega = (0, L) \times (-1, 1)$ with the following special spatial symmetries:

$$\begin{aligned} u_1(x_1, x_2) &= u_1(x_1, -x_2), & u_2(x_1, x_2) &= -u_2(x_1, -x_2), \\ p(x_1, x_2) &= p(x_1, -x_2), & \theta(x_1, x_2) &= -\theta(x_1, -x_2), \end{aligned}$$

for $(x_1, x_2) \in \Omega$. As a result of this symmetry, we observe that smooth enough functions satisfy

$$u_2, \theta, \frac{\partial u_1}{\partial x_2} = 0, \quad \text{for } x_2 = -1, 0, 1. \quad (2.3)$$

2.1. Function spaces. We will use the same notation indiscriminately for both scalar and vector Lebesgue and Sobolev spaces, which should not be a source of confusion. We denote

$$(u, v) := \int_{\Omega} u \cdot v, \quad \text{for } u, v \in L^2(\Omega),$$

$$((u, v)) := \int_{\Omega} \nabla u \cdot \nabla v, \quad \text{for } u, v \in H^1(\Omega),$$

and

$$|u| := (u, u)^{1/2}, \quad \|u\| := ((u, u))^{1/2}.$$

Note that $\|\cdot\|$ is not a norm unless we restrict the functions to some subspace. We define function spaces corresponding to the relevant physical boundary conditions as in [8], where

\mathcal{F}_1 is the set of trigonometric polynomials in (x_1, x_2) , with period L in the x_1 -variable, that are even, with period 2, in the x_2 -variable,

and

\mathcal{F}_2 is the set of trigonometric polynomials in (x_1, x_2) , with period L in the x_1 -variable, that are odd, with period 2, in the x_2 -variable.

The space of smooth vector-valued functions which incorporates the divergence-free condition shall be denoted by

$$\mathcal{V} := \{u \in \mathcal{F}_1 \times \mathcal{F}_2 : \nabla \cdot u = 0\}.$$

We denote the closures of \mathcal{V} and \mathcal{F}_2 in $L^2(\Omega)$ by H_0 and H_1 , respectively, which are endowed with the usual inner products

$$(u, v)_{H_0} := (u, v), \quad (\psi, \phi)_{H_1} := (\psi, \phi)$$

and the associated norms

$$\|u\|_{H_0} := (u, u)^{1/2}, \quad \|\psi\|_{H_1} := (\psi, \psi)^{1/2}.$$

Finally, we denote the closures of \mathcal{V} and \mathcal{F}_2 in $H_{per}^1(\Omega)$ by V_0 and V_1 respectively, endowed with the inner products

$$((u, v))_{V_0} := \frac{1}{|\Omega|}(u, v) + ((u, v)), \quad ((\psi, \phi))_{V_1} := ((\psi, \phi)),$$

and associated norms

$$\|u\|_{V_0} := \left(\frac{1}{|\Omega|} |u|^2 + \|u\|^2 \right)^{1/2}, \quad \|\phi\|_{V_1} := \|\phi\|,$$

where $|\Omega| = 2L$ is the volume of Ω .

2.2. The linear operators A_i . Let $D(A_0) = V_0 \cap H_{per}^2(\Omega)$ and $D(A_1) = V_1 \cap H_{per}^2(\Omega)$. Let $A_i : D(A_i) \rightarrow H_i$ ($i = 0, 1$) be the unbounded linear operators defined by

$$(A_i \phi, \psi)_{H_i} = ((\phi, \psi)), \quad \phi, \psi \in D(A_i).$$

Due to periodic boundary conditions, we have $A_i = -\Delta$. The operator A_0 is a nonnegative operator and possesses a sequence of eigenvalues with

$$0 = \lambda_{0,1} \leq \lambda_{0,2} \leq \dots \leq \lambda_{0,m} \leq \dots,$$

associated with an orthonormal basis $\{w_{0,m}\}_{m \in \mathbb{N}}$ of H_0 . The operator A_1 is a positive self-adjoint operator and possesses a sequence of eigenvalues with

$$0 < \lambda_{1,1} \leq \lambda_{1,2} \leq \dots \leq \lambda_{1,m} \leq \dots,$$

associated with an orthonormal basis $\{w_{1,m}\}_{m \in \mathbb{N}}$ of H_1 . Observe that we have the Poincaré inequality for temperature:

$$\begin{aligned} |\theta|^2 &\leq \lambda_1^{-1} \|\theta\|^2, \quad \forall \theta \in V_1, \\ \|\theta\|^2 &\leq \lambda_1^{-1} |A_1 \theta|^2, \quad \forall \theta \in D(A_1), \end{aligned}$$

where $\lambda_1 = \lambda_{1,1} = \pi^2 \min(1/4, L^{-2})$.

2.3. The bilinear maps B_i . Denote the dual space of V_i by V_i' ($i = 0, 1$). Define the bilinear map $B_0 : V_0 \times V_0 \rightarrow V_0'$ (and the trilinear map $b_0 : V_0 \times V_0 \times V_0' \rightarrow \mathbb{R}$) by the continuous extension of

$$b_0(u, v, w) := \langle B_0(u, v), w \rangle_{V_0'} = ((u \cdot \nabla)v, w), \quad u, v, w \in \mathcal{V}.$$

Define the scalar analogue $B_1 : V_0 \times V_1 \rightarrow V_1'$ (and the trilinear map $b_1 : V_0 \times V_1 \times V_1' \rightarrow \mathbb{R}$) by the continuous extension of

$$b_1(u, \theta, \phi) := \langle B_1(u, \theta), \phi \rangle_{V_1'} = ((u \cdot \nabla)\theta, \phi), \quad u \in \mathcal{V}, \quad \theta, \phi \in \mathcal{F}_2.$$

The bilinear maps B_i (and the trilinear maps b_i), $i = 0, 1$, have the orthogonality property:

$$b_0(u, v, v) = 0, \quad b_1(u, \theta, \theta) = 0, \quad u, v \in V_0, \quad \theta \in V_1. \quad (2.4)$$

Furthermore, due to periodicity on Ω , i.e., since $A_0 = -\Delta$, we have

$$b_0(u, u, A_0 u) = 0, \quad \forall u \in D(A_0), \quad (2.5)$$

as well as

$$b_0(v, v, A_0 w) + b_0(v, w, A_0 v) + b_0(w, v, A_0 v) = 0, \quad \forall v, w \in D(A_0), \quad (2.6)$$

(see, e.g., [17] for (2.5), [9] for (2.6)).

2.4. Functional setting. Following [10], we have the functional form of the RB problem (2.1):

$$\frac{du}{dt} + \nu A_0 u + B_0(u, u) = \mathbb{P}_\sigma(\theta e_2), \quad (2.7a)$$

$$\frac{d\theta}{dt} + \kappa A_1 \theta + B_1(u, \theta) = u \cdot e_2, \quad (2.7b)$$

$$u(0; x) = u_0(x), \quad \theta(0; x) = \theta_0(x), \quad (2.7c)$$

where \mathbb{P}_σ denotes the Leray projector.

3. STATEMENT OF RESULT

Theorem 3.1. The Rayleigh-Bénard problem (2.1) with stress-free boundary conditions (2.3) has a global attractor \mathcal{A}_α within the invariant affine space

$$W_\alpha = \{(u, \theta) \in V_0 \times V_1 : \int_\Omega u_1(x, t) \, dx = \alpha\} .$$

The elements in \mathcal{A}_α satisfy

$$|u|^2 \leq \frac{|\Omega|}{\nu^2 \lambda_1^2} + \alpha^2 |\Omega| , \quad (3.1)$$

$$\|u\|^2 \leq z_{\max} := \frac{|\Omega|}{\nu^2 \lambda_1} , \quad (3.2)$$

$$\|\theta\|^2 \lesssim \vartheta_{\max} := \lambda_1 z_{\max}^2 Pr^2 + z_{\max} Pr , \quad (3.3)$$

$$|A_0 u|^2 \leq f(\|u\|^2) \lesssim q_{\max} := \frac{z_{\max}^2}{\nu^2} + \frac{z_{\max}^{1/2}}{\nu} \vartheta_{\max}^{1/2} , \quad (3.4)$$

$$|A_1 \theta|^2 \leq g(\|\theta\|^2) \lesssim \eta_{\max} := \frac{z_{\max} \vartheta_{\max}}{\kappa^2} + \frac{q_{\max}^{2/3} \vartheta_{\max}}{\kappa^{4/3} \lambda_1^{1/3}} + \frac{z_{\max}}{\kappa^2 \lambda_1} , \quad (3.5)$$

where the functions f, g are defined below in (4.28), (4.35), respectively and Pr is the Prandtl number ν/κ .

Regions that bound the global attractor in the enstrophy, palinstrophy- and $\|\theta\|^2, |A_1 \theta|^2$ -planes are depicted in Figures 1, 2, below.

4. A PRIORI ESTIMATES

Global existence and uniqueness follows by the standard Galerkin procedure based on the trigonometric basis functions in the definitions of \mathcal{F}_1 and \mathcal{F}_2 . We thus proceed with *a priori* estimates.

4.1. L^2 bound on temperature. A variant of the maximum principle for temperature proved in Lemma 2.1 of [10] applies to stress-free boundary conditions. As a consequence for each strong solution (u, θ) of (2.7)

$$|\theta(t)| \leq |\Omega|^{1/2} + \Theta_0 e^{-\kappa t} , \quad (4.1)$$

where $|\Omega|$ is the volume of Ω and

$$\Theta_0 = |(\theta(0) - 1)_+| + |(\theta(0) + 1)_-|$$

4.2. L^2 bounds on velocity. We denote the space average of the horizontal velocity over the extended domain by

$$\alpha(t) = \frac{1}{|\Omega|} \int_\Omega u_1(x, t) \, dx .$$

From (2.1) and the periodic boundary conditions on Ω , we find that the spatial average of velocity is conserved, i.e., $d\alpha/dt = 0$. It follows that $u_\alpha = u - \alpha e_1$ satisfies

$$\frac{du_\alpha}{dt} + \nu A_0 u_\alpha + B_0(u_\alpha + \alpha e_1, u_\alpha) = \theta e_2 .$$

Since u_α has zero average, it satisfies the Poincaré inequality

$$\lambda_1 |u_\alpha|^2 \leq \|u_\alpha\|^2 . \quad (4.2)$$

Note that u_2 also satisfies a Poincaré inequality

$$\lambda_1 |u_2|^2 \leq \|u_2\|^2 , \quad (4.3)$$

but u_1 does not. Taking the scalar product with u_α , and applying (2.4), the Cauchy-Schwarz, Young inequalities as well as (4.2), we get

$$\frac{1}{2} \frac{d}{dt} |u_\alpha|^2 + \nu \|u_\alpha\|^2 \leq \frac{1}{2\nu\lambda_1} |\theta|^2 + \frac{\nu\lambda_1}{2} |u_\alpha|^2 \leq \frac{|\theta|^2}{2\nu\lambda_1} + \frac{\nu}{2} \|u_\alpha\|^2 .$$

Applying (4.2) once again, together with (4.1) and Young's inequality, we have

$$\frac{d}{dt} |u_\alpha|^2 + \nu\lambda_1 |u_\alpha|^2 \leq \frac{1}{\nu\lambda_1} (|\Omega| + \Theta_0^2 e^{-2\kappa t}) ,$$

so that

$$|u_\alpha(t)|^2 \leq e^{-\nu\lambda_1 t} |u_\alpha(0)|^2 + \frac{1}{\nu\lambda_1} \int_0^t (|\Omega| + \Theta_0^2 e^{-2\kappa s}) e^{\nu\lambda_1(s-t)} ds , \quad (4.4)$$

and thus,

$$\limsup_{t \rightarrow \infty} |u(t)|^2 \leq \frac{|\Omega|}{\nu^2 \lambda_1^2} + \alpha^2 |\Omega| . \quad (4.5)$$

4.3. An enstrophy bound. We note that ∇u has zero average over Ω by the periodicity of u . As a consequence, we have the Poincaré inequality

$$\lambda_1 \|u\|^2 \leq |A_0 u|^2 . \quad (4.6)$$

Taking the scalar product of (2.7a) with $A_0 u$, we have by the orthogonality property (2.5)

$$\begin{aligned} \frac{1}{2} \frac{d}{dt} \|u\|^2 + \nu |A_0 u|^2 &\leq |(\theta e_2, A_0 u)| \\ &\leq |\theta| |A_0 u| \leq \frac{1}{2\nu} |\theta|^2 + \frac{\nu}{2} |A_0 u|^2 , \end{aligned} \quad (4.7)$$

hence, by (4.1) and (4.6) we have

$$\frac{d}{dt} \|u\|^2 + \nu\lambda_1 \|u\|^2 \leq \frac{1}{\nu} (|\Omega| + \Theta_0^2 e^{-2\kappa t}) ,$$

and thanks to the Gronwall inequality we obtain

$$\limsup_{t \rightarrow \infty} \|u(t)\|^2 \leq z_{\max} := \frac{|\Omega|}{\nu^2 \lambda_1} . \quad (4.8)$$

Similar to the no-slip case analyzed in [10, 17], if $\|u(0)\| \leq M_1$, $\|\theta(0)\| \leq M_2$, and $\varepsilon > 0$ we have from (4.1), (4.5) and (4.8) that there exists $t_0 = t_0(M_1, M_2, \varepsilon)$ such that

$$|\theta(t)|^2 \leq |\Omega| + \varepsilon , \quad \forall t \geq t_0 , \quad (4.9)$$

$$|u(t)|^2 \leq \frac{|\Omega|}{\nu^2 \lambda_1^2} + \alpha^2 |\Omega| + \varepsilon , \quad \forall t \geq t_0 \quad (4.10)$$

$$\|u(t)\|^2 \leq \frac{|\Omega|}{\nu^2 \lambda_1} + \varepsilon , \quad \forall t \geq t_0 . \quad (4.11)$$

4.4. Bound on the temperature gradient. We start by taking the scalar product of (2.7b) with $A_1\theta = -\Delta\theta$, integrating by parts and applying the Cauchy-Schwarz and Young inequalities

$$\frac{1}{2} \frac{d}{dt} \|\theta\|^2 + \kappa |A_1\theta|^2 \leq |(B_1(u, \theta), A_1\theta)| + \frac{|u_2|^2}{\kappa} + \frac{\kappa}{4} |A_1\theta|^2. \quad (4.12)$$

We apply integration by parts to rewrite the trilinear term as

$$\begin{aligned} (B_1(u, \theta), A_1\theta) &= - \sum_{i,j=1}^2 \int_{\Omega} u_i \partial_i \theta \partial_j^2 \theta \, dx \\ &= \sum_{i,j=1}^2 \int_{\Omega} u_i \partial_{ij} \theta \partial_j \theta \, dx + \sum_{i,j=1}^2 \int_{\Omega} \partial_j u_i \partial_i \theta \partial_j \theta \, dx. \end{aligned}$$

We then use the chain rule to rewrite the first sum, again apply integration by parts, and then incompressibility to find

$$\begin{aligned} \sum_{i,j=1}^2 \int_{\Omega} u_i \partial_{ij} \theta \partial_j \theta \, dx &= \frac{1}{2} \sum_{i,j=1}^2 \int_{\Omega} u_i \partial_i (\partial_j \theta)^2 \, dx \\ &= -\frac{1}{2} \int_{\Omega} (\partial_1 u_1 + \partial_2 u_2) [(\partial_1 \theta)^2 + (\partial_2 \theta)^2] \, dx = 0. \end{aligned} \quad (4.13)$$

From the above, together with the Hölder, Ladyzhenskaya and Young inequalities then give

$$\begin{aligned} |(B_1(u, \theta), A_1\theta)| &\leq 4 \|u\| \|\nabla \theta\|_{L^4}^2 \\ &\leq c_1 \|u\| \|\theta\| |A_1\theta| \\ &\leq \frac{c_1^2}{\kappa} (\|u\| \|\theta\|)^2 + \frac{\kappa}{4} |A_1\theta|^2. \end{aligned} \quad (4.14)$$

Now combine (4.12), (4.14) and the Poincaré inequality (4.3) so that

$$\frac{d}{dt} \|\theta\|^2 + \kappa |A_1\theta|^2 \leq \frac{2c_1^2}{\kappa} \|u\|^2 \|\theta\|^2 + \frac{2|u_2|^2}{\kappa} \leq \frac{2c_1^2}{\kappa} \|u\|^2 \|\theta\|^2 + \frac{2\|u\|^2}{\kappa\lambda_1}.$$

We note that by the Cauchy-Schwarz inequality and (4.1),

$$\|\theta\|^2 \leq |\theta| |A_1\theta| \leq |\Omega|^{1/2} |A_1\theta|,$$

so that

$$\frac{d}{dt} \|\theta\|^2 \leq -\frac{\kappa}{|\Omega|} \|\theta\|^4 + \frac{c_1}{\kappa} \|u\|^2 \|\theta\|^2 + \frac{2\|u\|^2}{\kappa\lambda_1}. \quad (4.15)$$

Let $R^2 = z_{\max} + \varepsilon$. From (4.11), (4.15) and Young's inequality, we have for all $t \geq t_0$

$$\begin{aligned} \frac{d}{dt} \|\theta\|^2 &\leq -\frac{\kappa}{|\Omega|} \|\theta\|^4 + \frac{2c_1^2}{\kappa} \|\theta\|^2 R^2 + \frac{2R^2}{\kappa\lambda_1} \\ &\leq -\frac{\kappa}{2|\Omega|} \|\theta\|^4 + \frac{2c_1^4}{2\kappa^3} |\Omega| R^4 + \frac{2R^2}{\kappa\lambda_1} \\ &\leq -\frac{\kappa}{2|\Omega|} (\|\theta\|^4 - K^4), \end{aligned}$$

where

$$K^4 = \frac{4c_1^4}{\kappa^4} |\Omega|^2 R^4 + \frac{4|\Omega|}{\kappa^2 \lambda_1} R^2 .$$

We claim that

$$\limsup_{t \rightarrow \infty} \|\theta(t)\|^2 \leq \left[\frac{4c_1^4}{\kappa^4} |\Omega|^2 z_{\max}^2 + \frac{4|\Omega|}{\kappa^2 \lambda_1} z_{\max} \right]^{1/2} . \quad (4.16)$$

To prove this we let $\varepsilon > 0$, as above, and consider two possibilities.

Case I: If $\|\theta(t)\|^2 \leq (1 + 4\varepsilon)^{1/2} K^2$, for all $t \geq t_0$, then clearly

$$\limsup_{t \rightarrow \infty} \|\theta(t)\|^2 \leq (1 + 4\varepsilon)^{1/2} K^2 , \quad \forall \varepsilon > 0 . \quad (4.17)$$

Case II: Suppose there exists $t_* \geq t_0$ such that $\|\theta(t_*)\|^2 \geq (1 + 4\varepsilon)^{1/2} K^2$. We would then have that

$$\frac{d}{dt} \|\theta\|^2 \leq -\frac{\kappa\varepsilon}{|\Omega|} K^4 , \quad \forall t \geq t_* \text{ such that } \|\theta(t)\|^2 \geq (1 + 2\varepsilon)^{1/2} K^2 .$$

We conclude that $\|\theta(t)\|^2$ is strictly decreasing at a rate faster than $-\kappa\varepsilon K^4 / (2|\Omega|)$ for all $t \geq t_*$ such that $\|\theta(t)\|^2 \geq (1 + 2\varepsilon)^{1/2} K^2$. In particular, there exists t_{**} , with $t_* < t_{**} < \infty$ such that $\|\theta(t_{**})\|^2 = (1 + 2\varepsilon)^{1/2} K^2$. Moreover, for all $t > t_{**}$ we have $\|\theta(t)\|^2 < (1 + 2\varepsilon)^{1/2} K^2$. As a result, we again obtain (4.17).

In either case we may now take $\varepsilon \rightarrow 0^+$ to conclude (4.16). Introducing the Prandtl number in (4.16) and applying the square root inside the brackets we arrive at the simpler bounding expression

$$\limsup_{t \rightarrow \infty} \|\theta(t)\|^2 \lesssim \vartheta_{\max} := \lambda_1 z_{\max}^2 Pr^2 + z_{\max} Pr .$$

Thus, the ball $\mathcal{B}_\alpha(\varepsilon) \subset V_0 \times V_1$, defined by

$$\mathcal{B}_\alpha(\varepsilon) := \left\{ (u, \theta) : \|u\|_{H^1}^2 \leq \frac{1 + \lambda_1}{\nu^2 \lambda_1^2} |\Omega| + \alpha^2 |\Omega| + 2\varepsilon , \quad \|\theta\|^2 \leq \vartheta_{\max} \right\} ,$$

is absorbing. This gives for each α the existence of a global attractor \mathcal{A}_α , within the invariant subspace of solutions (u, θ) where the spatial average of velocity is fixed at α . The global attractor is contained in $\mathcal{B}_\alpha(0)$.

4.5. Palinstrophy bound. To estimate palinstrophy on \mathcal{A}_α we follow [5] almost verbatim except that the effect of time independent forcing of the Navier-Stokes equations is played by the bound $\|\theta\|^2 \leq \vartheta_{\max}$. The other difference is that our velocity is not normalized as in [5]. For completeness, and in order to arrive at an overall bound in terms of ν, κ , we distill the essential argument here.

Returning to (4.7), we integrate by parts, and then apply the Cauchy-Schwarz inequality to get

$$- \|u\| \sqrt{\vartheta_{\max}} \leq \frac{1}{2} \frac{d}{dt} \|u\|^2 + \nu |A_0 u|^2 \leq \|u\| \sqrt{\vartheta_{\max}} , \quad \forall (u, \theta) \in \mathcal{A}_\alpha .$$

We denote

$$z = \|u\|^2 , \quad q = |A_0 u|^2 , \quad \zeta = |A_0^{3/2} u|^2 , \quad \vartheta = \|\theta\|^2 . \quad (4.18)$$

Then whenever

$$\|u\| \sqrt{\vartheta_{\max}} \leq \frac{\nu}{2} |A_0 u|^2 , \quad \text{equivalently} \quad q \geq \frac{2}{\nu} \sqrt{z \vartheta_{\max}} , \quad (4.19)$$

we have

$$-3\nu q \leq \frac{dz}{dt} \leq -\nu q. \quad (4.20)$$

Setting $w = A_0 u$ in (2.6) and applying Agmon's inequality, we have

$$|(B_0(u, u), A_0^2 u)| = |(B_0(A_0 u, u), A_0 u)| \leq c_2 |A_0 u|^2 \|u\|^{1/2} |A_0^{3/2} u|^{1/2}.$$

We next take the scalar product of (2.7a) with $A_0^2 u$, and integrate by parts to obtain

$$\begin{aligned} \frac{1}{2} \frac{d}{dt} |A_0 u|^2 + \nu |A_0^{3/2} u|^2 &\leq |(\theta, A_0^2 u)| + |(B_0(u, u), A_0^2 u)| \\ &\leq \|\theta\| |A_0^{3/2} u| + c_2 |A_0 u|^2 \|u\|^{1/2} |A_0^{3/2} u|^{1/2}. \end{aligned} \quad (4.21)$$

Note that by the Cauchy-Schwarz inequality

$$\zeta := |A_0^{3/2} u|^2 \geq \frac{|A_0 u|^4}{\|u\|^2} = \frac{q^2}{z} \geq \frac{4}{\nu^2} \vartheta_{\max} \quad (4.22)$$

in the region

$$\mathcal{R} := \left\{ (z, q) \mid q \geq \frac{2}{\nu} \sqrt{z \vartheta_{\max}} \right\}. \quad (4.23)$$

It follows that

$$\|\theta\| |A_0^{3/2} u| = \vartheta^{1/2} \zeta^{1/2} \leq \frac{\nu}{2} \zeta \quad \forall (z, q) \in \mathcal{R},$$

and hence, as in [5],

$$\frac{dq}{dt} \leq \psi(\zeta) := -\nu \zeta + 2c_2 q z^{1/4} \zeta^{1/4}. \quad (4.24)$$

To close the system (eliminate ζ) we find that the maximum of ψ is achieved at

$$\zeta_{\max} := \left(\frac{c_2}{2\nu} q z^{1/4} \right)^{4/3} \quad \text{with a value} \quad \psi_{\max} = 3\nu \zeta_{\max}.$$

We note that

$$\frac{q^2}{z} \geq \zeta_{\max} \quad \text{if and only if} \quad q \geq \left(\frac{c_2}{2\nu} z \right)^2$$

so that by (4.22)

$$\frac{dq}{dt} \leq \psi_{\max} = \frac{3}{\nu^{1/3}} \left(\frac{c_2}{2} q z^{1/4} \right)^{4/3} \quad \text{if} \quad q \leq \left(\frac{c_2}{2\nu} z \right)^2 \quad (4.25)$$

and

$$\frac{dq}{dt} \leq \psi(q^2/z) = -\nu \frac{q^2}{z} + 2c_2 q^{3/2} \quad \text{if} \quad q \geq \left(\frac{c_2}{2\nu} z \right)^2. \quad (4.26)$$

We see that

$$\frac{dq}{dt} \leq 0 \quad \text{if} \quad q \geq \left(\frac{2c_2}{\nu} z \right)^2 \quad \text{and} \quad q \geq \frac{2}{\nu} \sqrt{z \vartheta_{\max}}. \quad (4.27)$$

By considering the steepest descent possible below

$$q = \left(\frac{2c_2}{\nu} z \right)^2$$

and the most shallow ascent possible above this parabola, we find three bounding curves $q = f_j(z)$, $j = 1, 2, 3$, after solving, in order, three final value problems. The first combines the (positive) bound in (4.25) with the upper bound in (4.20)

$$\begin{aligned} \frac{dq}{dz} &= -3 \left(\frac{c_2}{2\nu} \right)^{4/3} (qz)^{1/3}, \quad \text{for } z_1 \leq z \leq z_0 = z_{\max} = \frac{|\Omega|}{\nu^2 \lambda_1} \\ q(z_0) &= q_0 := \frac{2}{\nu^2} z_{\max}^{1/2} \vartheta_{\max}^{1/2}. \end{aligned}$$

The second picks up where the first leaves off and combines the (positive) bound in (4.26) with the upper bound in (4.20)

$$\begin{aligned} \frac{dq}{dz} &= \frac{q}{z} - \frac{2c_2}{\nu} q^{1/2}, \quad \text{for } z_2 \leq z \leq z_1 \\ q(z_1) &= q_1, \end{aligned}$$

while the third combines the (negative) bound in (4.26) with the *lower* bound in (4.20)

$$\begin{aligned} \frac{dq}{dz} &= \frac{q}{3z} - \frac{2c_2}{3\nu} q^{1/2}, \quad \text{for } 0 \leq z \leq z_2 \\ q(z_2) &= q_2, \end{aligned}$$

where q_1, q_2 are determined by the intersections of f_1 and f_2 (defined below) with the parabolas

$$q = \left(\frac{c_2}{2\nu} z \right)^2 \quad \text{and} \quad q = \left(\frac{2c_2}{\nu} z \right)^2$$

respectively. This results in a convex function in z

$$f_1(z) := \left[\frac{3}{2} \left(\frac{c_2}{2\nu} \right)^{4/3} \left(z_0^{4/3} - z^{4/3} \right) + q_0^{2/3} \right]^{3/2}$$

and concave functions in z

$$\begin{aligned} f_2(z) &:= \frac{1}{\nu^2} \left[-2c_2 z + \left(\nu q_1^{1/2} + 2c_2 z_1 \right) \left(\frac{z}{z_1} \right)^{1/2} \right]^2, \\ f_3(z) &:= \frac{1}{25\nu^2} \left[-6c_2 z + \left(5\nu q_2^{1/2} + 6c_2 z_2 \right) \left(\frac{z}{z_2} \right)^{1/6} \right]^2. \end{aligned}$$

A qualitative sketch of these three curves is shown in Figure 1. It is shown in [5] that the curve $q = f_3(z)$ does not intersect the curve $q = 2\sqrt{z\vartheta_{\max}}/\nu$. Let

$$f(z) := \begin{cases} f_1(z) & \text{if } z_1 \leq z \leq z_{\max} \\ f_2(z) & \text{if } z_2 \leq z < z_1 \\ f_3(z) & \text{if } 0 \leq z \leq z_2. \end{cases} \quad (4.28)$$

To prove (3.4), suppose there is an element in \mathcal{A}_α such that $q(0) > f(z(0))$. The solution through any element in \mathcal{A}_α exists for all negative time. If $q(t) > f(z(t))$ for all $t < 0$, since $q(t)$ increases with negative time, as long as $z(t) < z_2$, we have $q(t) > \min\{q(0), q_0\}$. By the upper bound in (4.20), $z(t)$ would then exceed z_2 in finite negative time. Thus, we must have $q(t) \leq f(z(t))$ at some $t < 0$. But forward in time, the region $q \leq f(z)$ is invariant, contradicting the assumption that the initial condition satisfied $q(0) > f(z(0))$.

We now find an overall bound on palinstrophy in \mathcal{A}_α . A straightforward calculation shows that substituting

$$q_1 = \left(\frac{c_2 z_1}{2\nu}\right)^2 \quad \text{into} \quad q_2 = f_2(z_2) = \left(\frac{2c_2 z_2}{\nu}\right)^2$$

reduces to

$$z_2 = \frac{25}{64} z_1.$$

Similarly, using

$$q_0 = \frac{2}{\nu} \sqrt{z_0 \vartheta_{\max}} \quad \text{in} \quad q_1 = f_1(z_1) = \left(\frac{c_2 z_1}{2\nu}\right)^2,$$

leads to

$$z_1 \leq \left[\frac{3}{2} z_0^{4/3} + \frac{4\nu^{2/3}}{c_2^{4/3}} z_0^{1/3} \vartheta_{\max}^{1/3} \right]^{3/4} \lesssim z_{\max} + \nu^{1/2} z_{\max}^{1/4} \vartheta_{\max}^{1/4}$$

so that

$$|A_0 u|^2 \leq q_2 \lesssim q_{\max} := \frac{z_{\max}^2}{\nu^2} + \frac{z_{\max}^{1/2}}{\nu} \vartheta_{\max}^{1/2}. \quad (4.29)$$

4.6. A bound on $|A_1 \theta|$. From (4.12) and (4.14) we have

$$-\frac{c_3}{\kappa} \|u\|^2 \|\theta\|^2 - \frac{2\|u\|^2}{\kappa \lambda_1} \leq \frac{d}{dt} \|\theta\|^2 + \kappa |A_1 \theta|^2 \leq \frac{c_3}{\kappa} \|u\|^2 \|\theta\|^2 + \frac{2\|u\|^2}{\kappa \lambda_1}.$$

Thus, if

$$|A_1 \theta|^2 \geq \frac{2}{\kappa^2} \left(c_3 \|u\|^2 \|\theta\|^2 + \frac{2\|u\|^2}{\lambda_1} \right),$$

it follows that

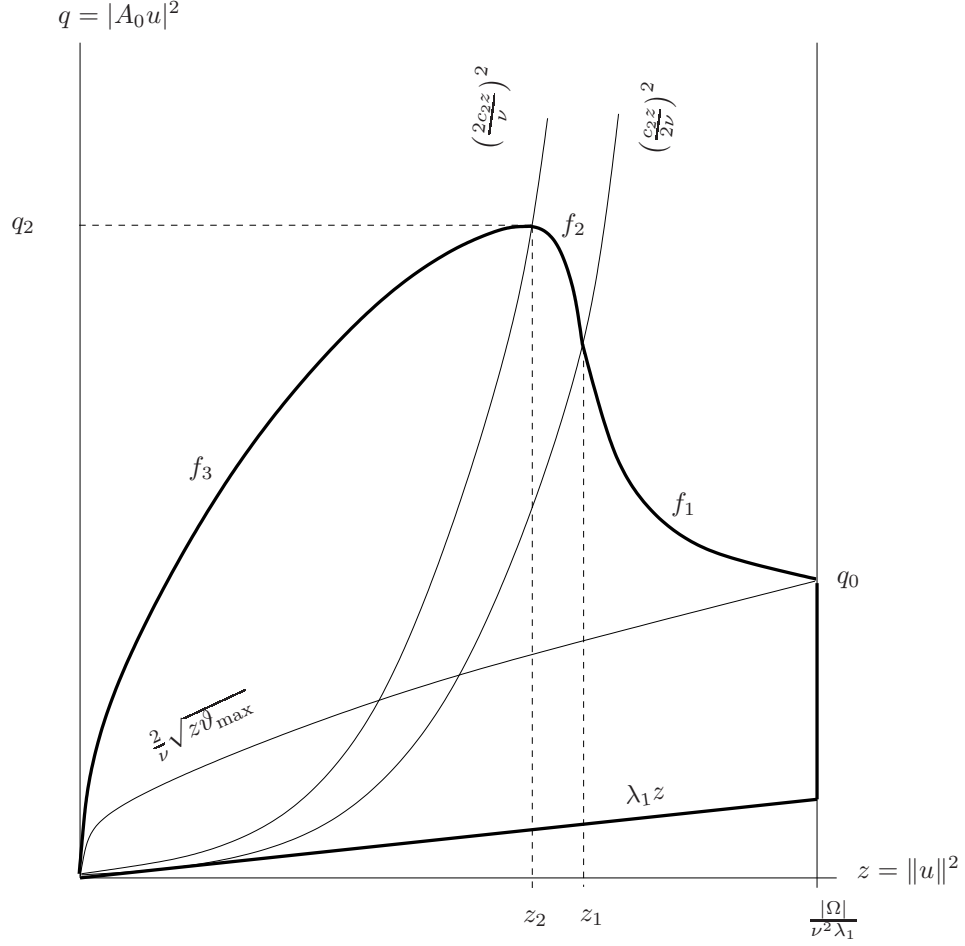
$$-\frac{3}{2} \kappa |A_1 \theta|^2 \leq \frac{d}{dt} \|\theta\|^2 \leq -\frac{1}{2} \kappa |A_1 \theta|^2. \quad (4.30)$$

We next take the scalar product of the temperature equation with $A_1^2 \theta = \Delta^2 \theta$ and using the fact that $A_0 u = -\Delta u$, write

$$\frac{1}{2} \frac{d}{dt} |A_1 \theta|^2 + \kappa |A_1^{3/2} \theta|^2 \leq |A_0 u| |A_1 \theta| + |(B_1(u, \theta), A_1^2 \theta)|. \quad (4.31)$$

We need to move two derivatives in the trilinear term in order to ultimately obtain a bound for it in which the highest order norm is $|A_1^{3/2} \theta|$. We integrate by parts to write

$$\begin{aligned} (B_1(u, \theta), A_1^2 \theta) &= \sum_{i,j,k=1}^2 \int_{\Omega} u_i \partial_i \theta \partial_j^2 \partial_k^2 \theta \, dx \\ &= - \sum_{i,j,k=1}^2 \int_{\Omega} u_i \partial_{ij} \theta \partial_j \partial_k^2 \theta \, dx - \sum_{i,j,k=1}^2 \int_{\Omega} \partial_j u_i \partial_i \theta \partial_j \partial_k^2 \theta \, dx = I + II. \end{aligned}$$

FIGURE 1. Qualitative sketches of the curves bounding \mathcal{A}_α .

We then integrate the first summation by parts

$$I = \sum_{i,j,k=1}^2 \int_{\Omega} u_i \partial_i \partial_j^2 \theta \partial_k^2 \theta \, dx + \sum_{i,j,k=1}^2 \int_{\Omega} \partial_j u_i \partial_{i,j} \theta \partial_k^2 \theta \, dx = I_a + I_b$$

and split the resulting first summation as

$$I_a = \sum_{i,j=1}^2 \int_{\Omega} u_i \partial_i \partial_j^2 \theta \partial_j^2 \theta \, dx + \sum_{i,j \neq k=1}^2 \int_{\Omega} u_i \partial_i \partial_j^2 \theta \partial_k^2 \theta \, dx = I_{a_1} + I_{a_2}$$

Proceeding as in (4.13), we find that $I_{a_1} = 0$. Integrating by parts again, we have

$$I_{a_2} = - \sum_{i,j \neq k=1}^2 \int_{\Omega} \partial_i u_i \partial_j^2 \theta \partial_k^2 \theta \, dx - \sum_{i,j \neq k=1}^2 \int_{\Omega} u_i \partial_j^2 \theta \partial_i \partial_k^2 \theta \, dx .$$

Since the first sum is zero by incompressibility, we have by symmetry that $I_{a_2} = -I_{a_2}$, and thus $I_{a_2} = 0$. Integrating by parts one more time, we have

$$II = \sum_{i,j,k=1}^2 \int_{\Omega} \partial_j^2 u_i \partial_i \theta \partial_k^2 \theta \, dx + I_b .$$

After gathering what remains, we use Agmon's and Ladyzhenskaya's inequalities to estimate the trilinear term as

$$\begin{aligned} |(B_1(u, \theta), A_1^2 \theta)| &= \left| \sum_{i,j,k=1}^2 \int_{\Omega} \partial_j^2 u_i \partial_i \theta \partial_k^2 \theta \, dx + 2 \sum_{i,j,k=1}^2 \int_{\Omega} \partial_j u_i \partial_{i,j} \theta \partial_k^2 \theta \, dx \right| \\ &\leq c |A_0 u| \|\theta\|^{1/2} |A_1^{3/2} \theta|^{1/2} |A_1 \theta| + c \|u\|^{1/2} |A_0 u|^{1/2} \|\theta\|_{H^2} |A_1 \theta|^{1/2} |A_1^{3/2} \theta|^{1/2} \\ &\leq c_4 |A_0 u| \frac{|A_1 \theta|^{3/2}}{\lambda_1^{1/4}} |A_1^{3/2} \theta|^{1/2} = \frac{c_4}{\lambda_1^{1/4}} q^{1/2} \eta^{3/4} \xi^{1/4} , \end{aligned}$$

where $\eta = |A_1 \theta|^2$, $\xi = |A_1^{3/2} \theta|^2$ and for convenience in what follows, we take $c_4 = 2 \max(c, c_3)$.

Using this in (4.31), we find

$$\begin{aligned} \frac{1}{2} \frac{d}{dt} |A_1 \theta|^2 + \kappa |A_1^{3/2} \theta|^2 &\leq |A_0 u| |A_1 \theta| + \frac{c_4}{\lambda_1^{1/4}} |A_0 u| |A_1 \theta|^{3/2} |A_1^{3/2} \theta|^{1/2} \\ &\leq \frac{2c_4}{\lambda_1^{1/4}} |A_0 u| |A_1 \theta|^{3/2} |A_1^{3/2} \theta|^{1/2} . \end{aligned}$$

Thus, invoking our palinstrophy bound q_{\max} , we have

$$\frac{d}{dt} \eta \leq \Phi(\xi) := -2\kappa \xi + \frac{4c_4}{\lambda_1^{1/4}} q_{\max}^{1/2} \eta^{3/4} \xi^{1/4} .$$

We find that

$$\Phi(\xi) \leq \Phi_{\max} = \frac{2}{\kappa^{1/3}} \left(\frac{c_4}{2\lambda_1^{1/4}} \right)^{4/3} q_{\max}^{2/3} \eta$$

and that

$$\Phi(\xi) \leq 0 \quad \forall \xi \geq \xi^* := \gamma \eta , \quad \text{where } \gamma := \left(\frac{2c_4}{\kappa \lambda_1^{1/4}} \right)^{4/3} q_{\max}^{2/3} .$$

In terms of z_0 , our enstrophy bound on the attractor, (4.30) holds for

$$\eta \geq g_3(\vartheta) := \frac{z_{\max}}{\kappa^2} \left(c_4 \vartheta + \frac{4}{\lambda_1} \right) . \quad (4.32)$$

Once again, by the Cauchy-Schwarz inequality, we have

$$|A_1^{3/2} \theta| \geq \frac{|A_1 \theta|^2}{\|\theta\|} , \quad \text{i.e., } \xi \geq \frac{\eta^2}{\vartheta} .$$

Thus for

$$\frac{\eta^2}{\vartheta} \leq \xi^* , \quad \text{equivalently } \eta \leq \gamma \vartheta ,$$

we combine

$$\frac{d}{dt} \eta \leq \Phi_{\max} \quad \text{with} \quad \frac{d}{dt} \vartheta \leq -\frac{\kappa}{2} \vartheta \quad (4.33)$$

and solve

$$\frac{d\eta}{d\vartheta} = -\gamma_0, \quad \eta(\vartheta_{\max}) = \eta_0 := \frac{z_{\max}}{\kappa^2} \left(c_4 \vartheta_{\max} + \frac{4}{\lambda_1} \right), \quad \text{where } \gamma_0 = 4^{-1/3} \gamma$$

to find a straight-line solution

$$\eta = g_1(\vartheta) := \eta_0 - \gamma_0(\vartheta - \vartheta_{\max}).$$

We then find the intersection of this line with $\eta = \gamma\vartheta$ to be at (ϑ_1, η_1) , where

$$\vartheta_1 = \frac{c_4 z_{\max}/\kappa^2 + \gamma_0 \vartheta_{\max}}{\gamma + \gamma_0} + \frac{4z_{\max}}{\kappa^2 \lambda_1 (\gamma + \gamma_0)}, \quad \text{and } \eta_1 = \gamma \vartheta_1. \quad (4.34)$$

For $\eta \geq \gamma\vartheta$ we combine

$$\frac{d}{dt} \eta \leq \Phi(\eta^2/\vartheta) = -2\kappa \frac{\eta^2}{\vartheta} + \frac{4c_4}{\lambda_1^{1/4}} q_{\max}^{1/2} \frac{\eta^{5/4}}{\vartheta^{1/4}} \quad \text{with} \quad \frac{d}{dt} \vartheta \geq -\frac{3}{2} \kappa \eta$$

and solve

$$\frac{d\eta}{d\vartheta} = \frac{4}{3\vartheta} \eta - \frac{8c_4}{3\lambda_1^{1/4} \kappa} q_{\max}^{1/2} \frac{\eta^{1/4}}{\vartheta^{1/4}}$$

to find

$$\eta = g_2(\vartheta) := \left[\left(\frac{\vartheta}{\vartheta_1} \right) \eta_1^{1/4} + \tilde{\gamma} \left(\vartheta^{3/4} - \vartheta \vartheta_1^{-1/4} \right) \right]^{4/3},$$

where

$$\tilde{\gamma} = \frac{8c_4}{\lambda_1^{1/4} \kappa} q_{\max}^{1/2}.$$

As we argued in Section 4.5, if an element in the global attractor were to project in the ϑ, η -plane above

$$\eta = \max \{g_1(\vartheta), g_2(\vartheta), g_3(\vartheta)\}, \quad (4.35)$$

then by (4.33) the solution through it would, in finite negative time, have to enter the region below the curves in (4.35). Yet, this region is invariant. We conclude from (4.34) and (4.29) that we have an overall bound on the global attractor of

$$|A_1 \theta|^2 \leq \eta_1 \lesssim \eta_{\max} := \frac{z_{\max}}{\kappa^2} \vartheta_{\max} + \gamma \vartheta_{\max} + \frac{z_{\max}}{\kappa^2 \lambda_1}.$$

A qualitative sketch of the region bounding the global attractor in this plane is shown in Figure 2.

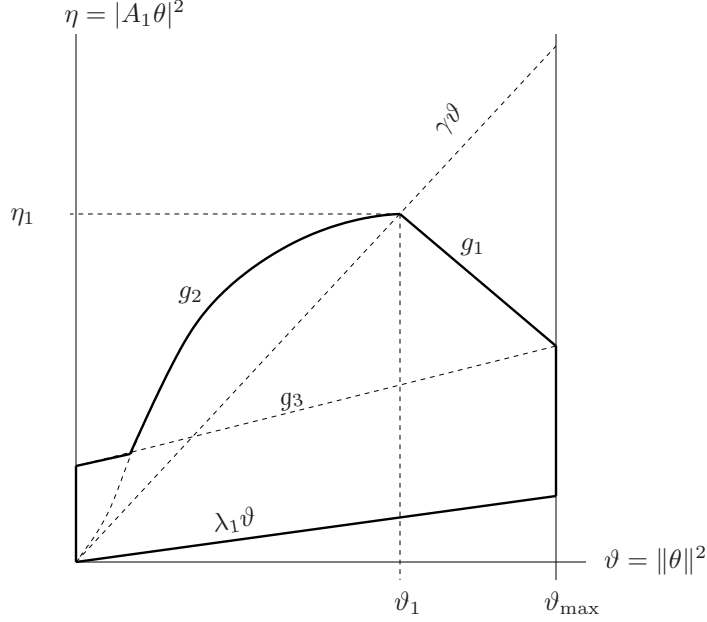
5. IMPLICATIONS FOR DATA ASSIMILATION

Suppose reality is represented by a particular solution to an evolution equation

$$\frac{dv}{dt} = F(v),$$

where the initial data $v(0)$ is *not* known. Instead continuous data of the form $I_h v(t)$ is known over an interval, $t \in [t_1, t_2]$, for a certain type of interpolating operator I_h with spatial resolution h . The nudging approach to data assimilation amounts to solving the auxiliary system

$$\frac{d\tilde{v}}{dt} = F(\tilde{v}) - \mu I_h(\tilde{v} - v), \quad (5.1)$$

FIGURE 2. Bounding region in the $\|\theta\|^2, |A_1\theta|^2$ -plane.

using *any* initial condition, e.g., $\tilde{v}_0 = 0$. It was shown in [2, 3] that if $\mu > 0$ is sufficiently large, and correspondingly, h sufficiently small, then, in some norm, $\|v(t) - \tilde{v}(t)\|_{\square} \rightarrow 0$ at an exponential rate, as $t \rightarrow \infty$. In fact, computations indicate that this approach works with data that is much more coarse than suggested by rigorous estimates (see [1, 6, 7, 11]). Flexibility in the choice of interpolant is one of the main advantages of injecting the observed data through a feedback nudging term, rather than into terms involving spatial derivatives [2, 14]. Numerical errors are shown to be bounded uniformly in time for semi-discrete [15] and fully discrete schemes [13] for (5.1).

Now consider this approach for the stress-free Rayleigh-Bénard system (2.7) using data from only the horizontal component of velocity. This means solving the auxiliary system

$$\begin{aligned} \frac{d\tilde{u}}{dt} + \nu A_0 \tilde{u} + B_0(\tilde{u}, \tilde{u}) &= \mathbb{P}_{\sigma}(\tilde{\theta} e_2) - \mu \mathbb{P}_{\sigma} I_h(\tilde{u}_1 - u_1) e_1, \\ \frac{d\tilde{\theta}}{dt} + \kappa A_1 \tilde{\theta} + B_1(\tilde{u}, \tilde{\theta}) &= \tilde{u} \cdot e_2, \\ \tilde{u}(0; x) &= 0, \quad \tilde{\theta}(0; x) = 0. \end{aligned}$$

It was proved in [8] that if $\mu h^2 \lesssim \nu$ and

$$\mu \geq K_1 \sim \frac{1}{\kappa \lambda_1} + \frac{1}{\nu \kappa^2} + \frac{1}{\kappa} + \frac{|A_0 u|^2}{\nu}, \quad (5.2)$$

then

$$\|u(t) - \tilde{u}(t)\| + |\theta(t) - \tilde{\theta}(t)| \rightarrow 0 \quad \text{as } t \rightarrow \infty$$

at an exponential rate. Also shown there was that if

$$\mu \geq K_2 \sim K_1 + \frac{1}{\kappa} \|\theta\|^2 |A_1 \theta|^2, \quad (5.3)$$

then the stronger convergence

$$\|u(t) - \tilde{u}(t)\| + \|\theta(t) - \tilde{\theta}(t)\| \rightarrow 0, \quad \text{as } t \rightarrow \infty,$$

holds at an exponential rate. The bounds in this paper on $\|\theta\|$, $|A_0 u|$ and $|A_1 \theta|$ are all algebraic, suggesting that data assimilation by nudging with just the horizontal velocity could be effective for the stress-free Rayleigh-Bénard system. We present computational evidence to this effect in the next section.

6. COMPUTATIONAL RESULTS

The computations presented below were done using Dedalus, an open-source package for solving partial differential equations using pseudo-spectral methods (see [4]). The time stepping is done by a four-stage third order Runge-Kutta method.

We solve (2.1) with $L = 2$ in the physical domain $\Omega_0 = (0, L) \times (0, 1)$. The physical parameters of viscosity and thermal diffusivity are related to the Rayleigh and Prandtl numbers through

$$\nu = \sqrt{\frac{Pr}{Ra}}, \quad \kappa = \frac{1}{\sqrt{Ra \cdot Pr}}.$$

We take $Pr = 1$ so that in our dimensionless variables $Ra := (\nu \kappa)^{-1} = \nu^{-2}$ and use n_F Fourier modes in the x_1 -direction and n_C Chebyshev modes in the x_2 -direction. The numbers of modes used are $n_F \times n_C = 256 \times 128, 1024 \times 512, \text{ and } 2048 \times 1024$ for runs at $Ra = 10^6, 10^7, 10^8$ respectively.

6.1. Sharpness. Each plot in Figure 3 shows the projection of a solution after a transient phase in a plane spanned by the norms bounded by our analysis. The solutions are plotted over the time period $200 \leq t \leq 1000$ for $Ra = 10^6, 10^7$ and over $200 \leq t \leq 1485$ for $Ra = 10^8$ (time units in the RB system (2.1)). The initial condition in each case is $(u_0, \theta_0) = (0, 0)$ so the average α of the horizontal velocity is zero.

It is not surprising that our rigorous overall bounds as well as the curves in Figures 1, 2 are orders of magnitude greater than the norms of these solutions. Plotting the bounds and curves together with the solutions is not revealing. Instead, to gauge a trend in sharpness, we plot in Figure 4 the ratios

$$\frac{z_{\max}}{\max_{\mathcal{A}} z}, \quad \frac{\vartheta_{\max}}{\max_{\mathcal{A}} \vartheta}, \quad \frac{q_{\max}}{\max_{\mathcal{A}} q}, \quad \frac{\eta_{\max}}{\max_{\mathcal{A}} \eta}. \quad (6.1)$$

The slopes of the ratios suggest, at least over this range of the Rayleigh number, that the bounds for $\|u\|^2, \|\theta\|^2$ are inflated by roughly a factors Ra and $Ra^{3/2}$, respectively. That the ratios for η and ϑ are nearly parallel from $Ra = 10^7$ to $Ra = 10^8$ is consistent with the factor of ϑ_{\max} in η_{\max} . A similar observation holds for shallower slope of the q ratio from $Ra = 10^7$ to $Ra = 10^8$ and the factor of $\vartheta_{\max}^{1/2}$ in q_{\max} .

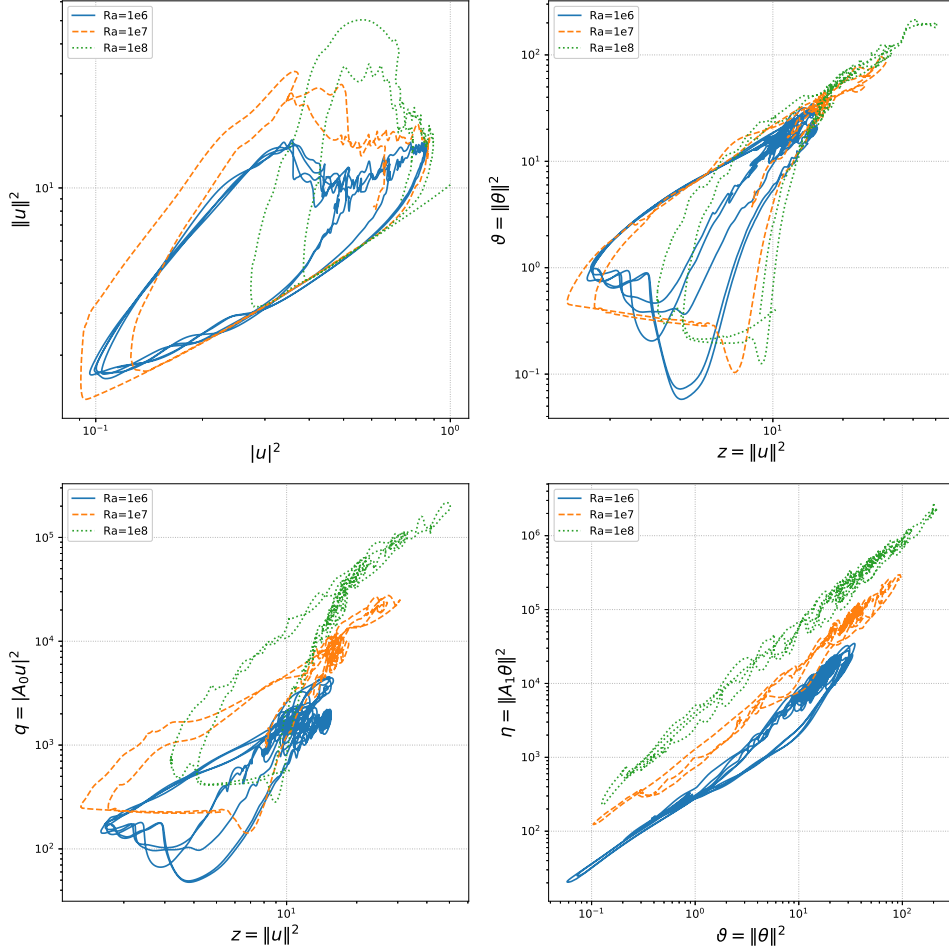


FIGURE 3. Projections after a transient period

6.2. Data assimilation. Nudging is carried out at $Ra = 10^6$ using the interpolant operator I_h at every m^{th} nodal value in each direction, i.e.,

$$h(m; n_F, n_C) = \max(h_F(m), h_C(m)),$$

where m is a positive integer, and

$$h_F(m) = \frac{mL}{n_F}, \quad h_C(m) = \max\{|x_2^{im} - x_2^{(i+1)m}| : i = 0, 1, \dots, \lfloor n_C/m \rfloor - 1\},$$

where (x_2^j) are the Chebyshev grid points in the x_2 -direction of the physical space. The nudging parameter is fixed at $\mu = 1$.

Figure 5 shows that at $h = h(16)$ the solution to the data assimilation system converges to the reference solution at an exponential rate. At $h = h(32)$ the error appears to saturate around 10^{-3} during rapid oscillations (see Figure 6). We found that at $h = h(64)$ the nudged solution does not converge to the reference at all (not shown). This demonstrates a critical value of h .

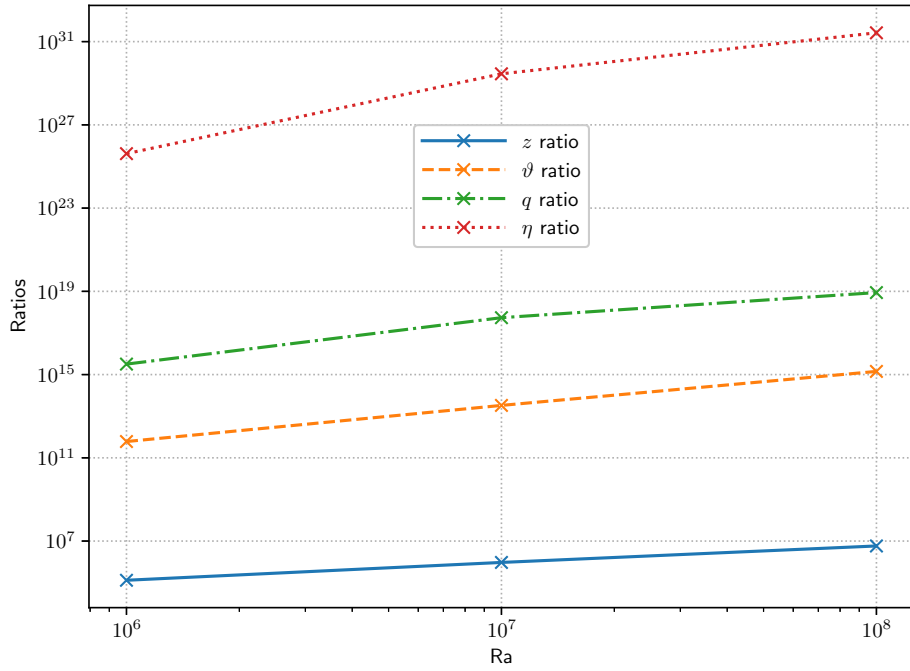


FIGURE 4. Ratios in (6.1)

Data assimilation by nudging works much more effectively than the rigorous analysis can guarantee. The value of μ and corresponding resolution h of the data suggested by the conditions (5.2) and (5.3) are based on compounded, conservative estimates derived using general inequalities which are not saturated by 2D convective flows. In addition, as demonstrated in (6.1), our algebraic rigorous estimates for $\|\theta\|$, $|A_0 u|$, and $|A_1 \theta|$ in this case of stress-free boundary conditions, though much better than the exponential bounds previously known, are still considerably artificially inflated. Numerical nudging tests in [7] for the Rayleigh-Bénard system with no-slip boundary conditions suggest that better bounds on the attractor might hold in that case as well, though proving that would require yet different techniques.

7. ACKNOWLEDGMENTS

The authors acknowledge the Indiana University Pervasive Technology Institute (see [16]) for providing HPC (Big Red II, Carbonate), storage resources that have contributed to the research results reported within this paper.

The work of Y. Cao was supported in part by National Science Foundation grant DMS-1418911, that of M.S. Jolly by NSF grant DMS-1818754. The work of E.S. Titi was supported in part by the Einstein Visiting Fellow Program, and by the John Simon Guggenheim Memorial Foundation. J.P. Whitehead acknowledges support from the Simon's Foundation through award number 586788, and the hospitality of the Department of Mathematics at Indiana University where part of this work was instigated.

REFERENCES

- [1] M. U. ALTAF, E. S. TITI, T. GEBRAEL, O. M. KNIO, L. ZHAO, M. F. MCCABE, AND I. HOTEIT, *Downscaling the 2D Bénard convection equations using continuous data assimilation*, *Comput. Geosci.*, 21 (2017), pp. 393–410.
- [2] A. AZOUANI, E. OLSON, AND E. S. TITI, *Continuous data assimilation using general interpolant observables*, *J. Nonlinear Sci.*, 24 (2014), pp. 277–304.
- [3] A. AZOUANI AND E. S. TITI, *Feedback control of nonlinear dissipative systems by finite determining parameters—a reaction-diffusion paradigm*, *Evol. Equ. Control Theory*, 3 (2014), pp. 579–594.
- [4] K. J. BURNS, G. M. VASIL, J. S. OISHI, D. LECOANET, AND B. BROWN, *Dedalus: Flexible framework for spectrally solving differential equations*. Astrophysics Source Code Library, Mar. 2016.
- [5] R. DASCALIUC, C. FOIAS, AND M. S. JOLLY, *Estimates on enstrophy, palinstrophy, and invariant measures for 2-D turbulence*, *J. Differential Equations*, 248 (2010), pp. 792–819.
- [6] P. C. DI LEONI, A. MAZZINO, AND L. BIFERALE, *Inferring flow parameters and turbulent configuration with physics-informed data assimilation and spectral nudging*, *Phys. Rev. Fluids*, 3 (2018), p. 104604.
- [7] A. FARHAT, H. JOHNSTON, M. JOLLY, AND E. S. TITI, *Assimilation of nearly turbulent Rayleigh-Bénard flow through vorticity or local circulation measurements: a computational study*, *J. Sci. Comput.*, 77 (2018), pp. 1519–1533.
- [8] A. FARHAT, E. LUNASIN, AND E. S. TITI, *Continuous data assimilation for a 2D Bénard convection system through horizontal velocity measurements alone*, *J. Nonlinear Sci.*, 27 (2017), pp. 1065–1087.
- [9] C. FOIAS, M. S. JOLLY, O. P. MANLEY, AND R. ROSA, *Statistical estimates for the Navier-Stokes equations and the Kraichnan theory of 2-D fully developed turbulence*, *J. Statist. Phys.*, 108 (2002), pp. 591–645.
- [10] C. FOIAS, O. MANLEY, AND R. TEMAM, *Attractors for the Bénard problem: existence and physical bounds on their fractal dimension*, *Nonlinear Anal.*, 11 (1987), pp. 939–967.
- [11] M. GESHO, E. OLSON, AND E. S. TITI, *A computational study of a data assimilation algorithm for the two-dimensional Navier-Stokes equations*, *Commun. Comput. Phys.*, 19 (2016), pp. 1094–1110.
- [12] D. GOLUSKIN, H. JOHNSTON, G. R. FLIERL, AND E. A. SPIEGEL, *Convectively driven shear and decreased heat flux*, *Journal of Fluid Mechanics*, 759 (2014), pp. 360–385.
- [13] H. A. IBDAB, C. F. MONDAINI, AND E. S. TITI, *Uniform in time error estimates for fully discrete numerical schemes of a data assimilation algorithm*, arXiv:1805.01595v1 [math.NA].
- [14] D. A. JONES AND E. S. TITI, *Determining finite volume elements for the 2D Navier-Stokes equations*, *Phys. D*, 60 (1992), pp. 165–174.
- [15] C. F. MONDAINI AND E. S. TITI, *Uniform-in-time error estimates for the postprocessing Galerkin method applied to a data assimilation algorithm*, *SIAM J. Numer. Anal.*, 56 (2018), pp. 78–110.
- [16] C. A. STEWART, V. WELCH, B. PLALE, G. FOX, M. PIERCE, AND T. STERLING, *Indiana University Pervasive Technology Institute*, <https://doi.org/10.5967/K8G44NGB>, (2017).

- [17] R. TEMAM, *Infinite-dimensional dynamical systems in mechanics and physics*, vol. 68 of Applied Mathematical Sciences, Springer-Verlag, New York, second ed., 1997.
- [18] J. P. WHITEHEAD AND C. R. DOERING, *Ultimate state of two-dimensional Rayleigh-Bénard convection between free-slip fixed-temperature boundaries*, Phys. Rev. Lett., 106 (2011), p. 244501.

¹DEPARTMENT OF MATHEMATICS, INDIANA UNIVERSITY, BLOOMINGTON, IN 47405

† CORRESPONDING AUTHOR

²DEPARTMENT OF MATHEMATICS, TEXAS A&M UNIVERSITY, 3368 TAMU, COLLEGE STATION, TX 77843-3368, USA. DEPARTMENT OF COMPUTER SCIENCE AND APPLIED MATHEMATICS, WEIZMANN INSTITUTE OF SCIENCE, REHOVOT 76100, ISRAEL. DEPARTMENT OF APPLIED MATHEMATICS AND THEORETICAL PHYSICS, UNIVERSITY OF CAMBRIDGE, CAMBRIDGE CB3 0WA, UK.

³DEPARTMENT OF MATHEMATICS, BRIGHAM YOUNG UNIVERSITY, PROVO, UT 84602

E-mail address, Y. Cao: `cao20@iu.edu`

E-mail address, M. S. Jolly: `msjolly@indiana.edu`

E-mail address, E. S. Titi: `titi@math.tamu.edu` and `Edriss.Titi@damtp.cam.ac.uk`

E-mail address, J. P. Whitehead: `whitehead@mathematics.byu.edu`

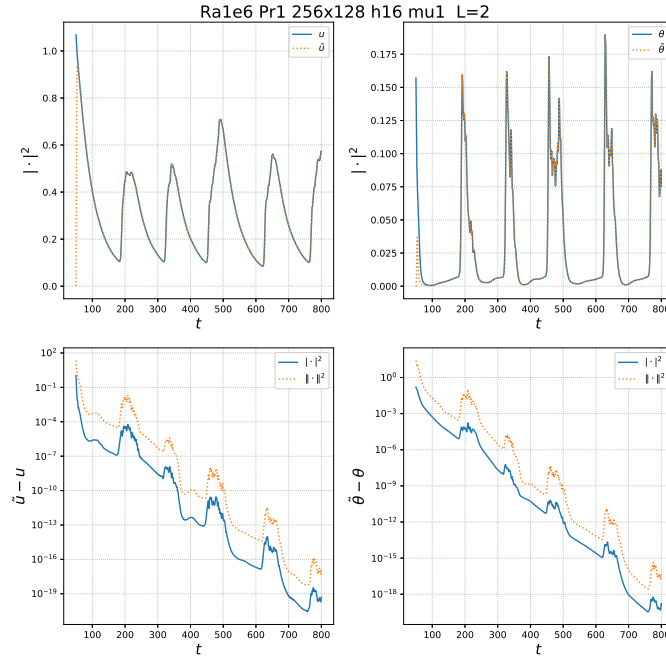


FIGURE 5. Data assimilation at $Ra = 10^6$ and $Pr = 1$ with $h(16)$.

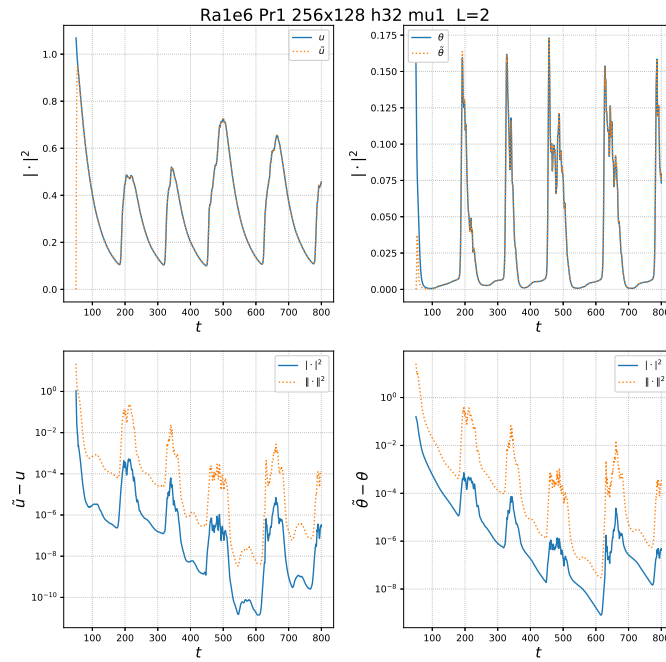


FIGURE 6. Data assimilation at $Ra = 10^6$ and $Pr = 1$ with $h(32)$.